

## MIT Open Access Articles

*Simulation and sensitivity analysis of controlling parameters in resistance spot welding*

The MIT Faculty has made this article openly available. **Please share** how this access benefits you. Your story matters.

**Citation:** Kim, Euiwhan, and Thomas W. Eagar. "Simulation and Sensitivity Analysis of Controlling Parameters in Resistance Spot Welding." *Metals and Materials International* 21, no. 2 (March 2015): 356–364.

**As Published:** <http://dx.doi.org/10.1007/s12540-015-4312-2>

**Publisher:** The Korean Institute of Metals and Materials

**Persistent URL:** <http://hdl.handle.net/1721.1/105532>

**Version:** Author's final manuscript: final author's manuscript post peer review, without publisher's formatting or copy editing

**Terms of use:** Creative Commons Attribution-Noncommercial-Share Alike



# Simulation and Sensitivity Analysis of Controlling Parameters in Resistance Spot Welding

Euiwhan Kim<sup>1,\*</sup> and Thomas W. Eagar<sup>2</sup>

<sup>1</sup>Department of Systems Engineering, Ajou University, Suwon 443-749, Korea

<sup>2</sup>Professor of Materials Engineering and Engineering Systems, Massachusetts Institute of Technology, Cambridge, MA02139, U.S.A.

(received date: 25 June 2014 / accepted date: 13 September 2014)

This study was performed to investigate the fundamental parameters controlling the nugget growth. The parameters were categorized into four groups, i.e. material parameters, electrical parameters, thermal parameters and geometrical parameters. In order to quantify the sensitivity of nugget growth to changes in these parameters, a numerical model which incorporates the electrical, mechanical and thermal contact was developed. As a result, a sensitivity index table was constructed and analyzed to ascertain the relative importance of these characteristic parameters. It was found that the most important factor in determining the variability of nugget growth behavior is the ratio of contact radius to electrode radius and the ratio of electrode radius to the square of specimen thickness. In general for a variation of 10%, the geometrical parameters are most important, followed by the material parameters. The electrical parameters and the thermal parameters are the least important. The importance of contact at the faying interface is greater for the contact area than for the contact resistance.

**Keywords:** metals, welding, interfaces, computer simulation, nugget growth

## 1. INTRODUCTION

To investigate the fundamental phenomena in the resistance spot welding process, the process system was qualitatively modeled in a separate research program and four groups of characteristic parameters were derived.[1,2] The four groups are the material parameters, geometrical parameters, electrical parameters and the thermal parameters. These parameters and the qualitative effects on the lobe width and the energy input is outlined in Table 1 [1]. Among these, some parameters are controllable while others are inherent to the system. The difficulties confronted in assessing the weldability of spot welding are mainly due to the combined effects of these parameters. Furthermore, there is some variability in each parameter from weld to weld. The material properties may not always be the same even though the material classification is the same. The electrode contact area and the surface condition of the electrode also changes during the welding sequence. All these uncertainties affect the weldability of a material to a greater or lesser extent, yet in most cases, it is very difficult to experimentally quantify the effect of variations in each parameter [3-9]. Even though various

numerical analyses were performed, there are few studies to investigate the controlling parameters of the process overall [10-16]. In this research, in order to investigate the sensitivity of nugget growth to changes in each parameter, a numerical model which incorporates the electrical, mechanical and thermal contact was developed and the simulation results were analyzed quantitatively to develop a fundamental understanding of the controlling parameters in the process.

## 2. NUMERICAL MODEL

An axisymmetric two dimensional model was developed using the ABAQUS code, a finite element computer algorithm. During welding three different physical processes occur simultaneously, i.e. thermal, electrical and mechanical processes are present. For accurate calculation of the nugget growth behavior all three physical processes must be incorporated simultaneously. The pressure for the mechanical contact model was a combination of electrode force and the thermal load. At first the contact area at room temperature was estimated from a mechanical model. Then a calculation of the temperature field with the thermal load was performed using the contact area obtained from the mechanical model. Even though the calculation shows plausible contact behavior, the true contact in the welding process can deviate from

\*Corresponding author: keuiwhan@ajou.ac.kr

**Table 1.** Effect of parameters on the lobe width and energy input (after Refs. 1, 2)

Increase in	Lobe Width	Energy Input
<b>MATERIAL PARAMETER</b>		
Thermal conductivity $k_b$	+	+
Bulk electrical Resistivity $\sigma_b$	-	-
Heat Capacity $\rho C_p$	+	+
$\rho C_p / \sigma_b$	+	+
$k_b / \sigma_b$	+	+
<b>GEOMETRIC PARAMETER</b>		
$b / L^2$	?	+
$D / b$	-	+
<b>ELECTRICAL PARAMETER</b>		
$R_c / R_b$	+	?
$R_c^f / R_c^e$	+	?
<b>THERMAL PARAMETER</b>		
$h_w / R$	+	+
$h_c / k_b$	+	+
$h_c / R$	+	+

Subscript  $c$  : contact  
 Subscript  $b$  : work piece  
 Subscript  $w$  : water cooling  
 Superscript  $f$  : faying interface  
 Superscript  $e$  : electrode  
 $b$  : electrode radius  
 $R$  : total electrical resistance  
 $L$  : specimen thickness  
 $D$  : contact radius at faying interface  
 $h$  : heat transfer coefficient

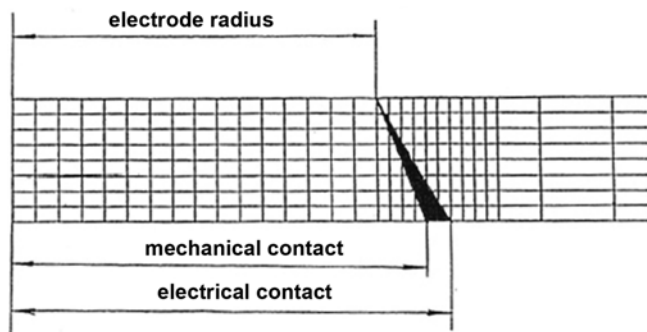


**Fig. 1.** Schematic comparison of the current flowing area and the mechanical contact area.

the model. For this reason, if the calculated nugget size did not match the experimentally measured nugget size, the contact area at the faying interface was modified until a closer match was obtained.

As for the thermal model, this model incorporates the redistribution of current density caused by the uneven temperature field and the size of the mechanical contact. Figure 1 shows a schematic of the current conducting area. Here the meaning of the contact size is somewhat different from the mechanical contact size calculated from the contact model. In this case the contact size is the area where the current can flow. For example, the current conducting area of a zinc coated material is different from the numerically calculated area due to the formation of a molten zinc halo around the weld nugget.

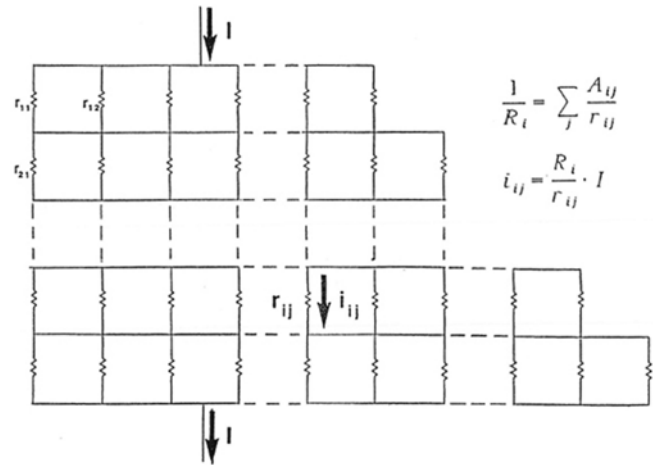


**Fig. 2.** Current flow model.

For a given contact area the welding current was redistributed at each time step. Figure 2 shows the concept of this current distribution scheme with a representative electrical circuit. In this way the model can consider differences in the temperature dependent electrical resistivity of different materials.

Even though the electrical resistivity of the copper electrode is one order of magnitude smaller than that of the steel, it was included in the analysis as the current density becomes higher near the contact tip [17]. Convective water cooling is assumed to have a fixed heat transfer coefficient of  $0.02 \text{ W/mm}^2 \text{ }^\circ\text{C}$ .

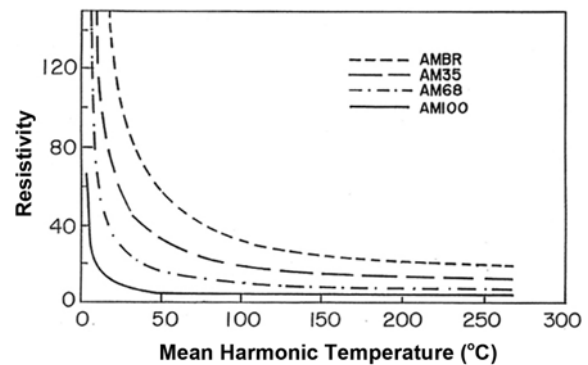


**Fig. 3.** Electrical contact resistivity at electrode interface (after Ref. 17).

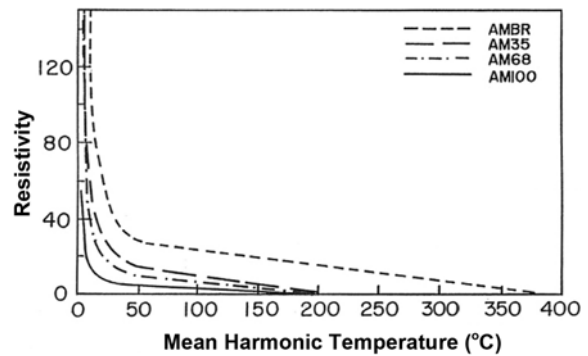


**Fig. 4.** Electrical contact resistivity at faying interface (after Ref. 17).

The electrical contact resistivity and the contact heat transfer coefficient at the electrode interface were taken from reference 18. The electrical contact resistivities are shown in Fig. 3 and Fig. 4 [18].

Temperature dependent properties such as bulk electrical resistivity, heat capacity, thermal conductivity, heat of fusion and electrical and thermal contact properties were used in this analysis. The values for these properties were varied according to both published and measured data.

The sheet steels used in these simulations and experiments are designated as follows. AMBR: bare steel, AM35: electrogalvanized with 35 g/sq. m of zinc per side, AM68: electrogalvanized with 68 g/sq. m of zinc per side, AM100: electrogalvanized with 100 g/sq. m of zinc per side, G40 and G60: hot dip galvanized.

### 3. RESULTS AND DISCUSSION

#### 3.1. Contact behavior

In general, at the start of welding, the location for the maximum contact pressure at both interfaces and the ratio of maximum pressure to average pressure is listed in Table 2. Table 2 also shows the contact size at the faying interface. The electrode force did not cause any significant change in contact size. Thus, it is seen that the electrode force has the most effect on the electrical and thermal contact properties rather than on the contact area during the early stages of welding. Table 2 lists the ratio of contact radius to the electrode

radius. The ratio is almost constant at 1.2. Thus the contact radius at the faying interface is 20% larger than the electrode face radius. This will result in 30% lower average current density at the faying interface than at the electrode interface. Thus, by the nature of mechanical contact the current density is much higher at the electrode interface. Table 4 shows the effect of specimen thickness on the contact area. As the specimen thickness increases, the ratio of contact radius to electrode radius increases. The increment of contact radius is proportional to the specimen thickness. Thus, it is seen that the electrode force has little effect on the contact size for a given material thickness. However, these results are applicable only to the very early stages of the welding.

Figures 5 and 6 show cascade plots of the contact pressure at the faying interface and at the electrode interface during welding. As welding progresses, the contact pressure at the center increases due to thermal expansion in the electrode and the work piece. In contrast, the contact pressure at both the periphery of the faying interface and the electrode interface decreases resulting in the loss of the mechanical seal. Due to the larger displacement in the center, the contact size at the faying interface decreases as shown in Fig. 7. This may be related to expulsion of weld metal.

As the electrode force increases, the contact size at the faying interface becomes larger as in Fig. 7. The force has a strong effect on the contact area at the faying interface particularly in the early stages of welding. A minimum contact area is observed when the nugget grows to a size comparable

**Table 2.** Effect of electrode force on contact size and pressure

Electrode force (lbs)	Radius for maximum contact pressure (mm)		Normalized maximum pressure		Contact size at faying interface, D (mm)
	Electrode interface	Faying interface	Electrode interface	Faying interface	
500	2.25	1.95	1.54	0.93	2.96
650	2.25	1.95	1.57	0.93	2.96
800	2.25	1.95	1.61	0.94	2.96

\*electrode radius : 2.4 mm

**Table 3.** Effect of electrode size on the contact size at faying interface

Electrode radius, b (mm)	Contact radius at faying interface, D (mm)	Ratio of contact radius to electrode radius
2.4	2.96	1.23
2.6	3.16	1.22
2.8	3.36	1.20

\*electrode force : 500lbs

**Table 4.** Effect of specimen thickness on the contact size

Specimen thickness, L (mm)	Contact radius at faying interface, D (mm)	Ratio of contact radius to electrode radius, D/b	Ratio of difference in contact radius and electrode radius to the specimen thickness
0.6	2.80	1.17	0.67
0.8	2.96	1.23	0.67
1.2	3.20	1.33	0.67
1.8	3.48	1.45	0.67

\*electrode radius : 2.4 mm, electrode force : 650 lbs

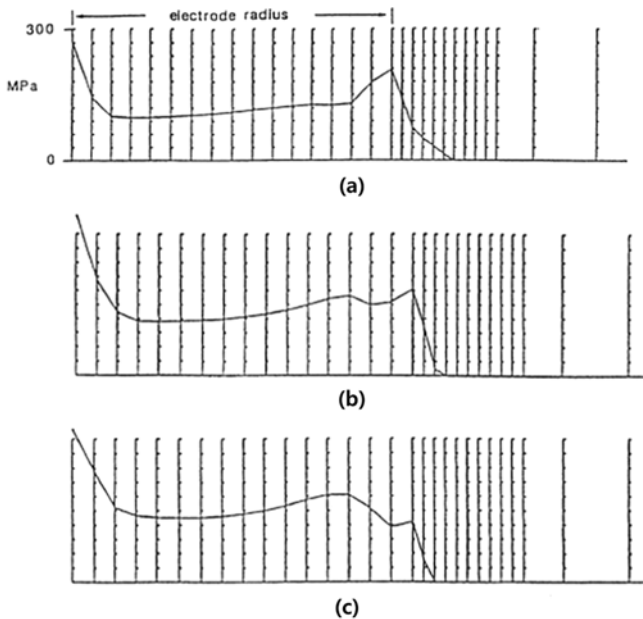


Fig. 5. Change of contact pressure at the faying interface during welding. (a) after 1 cycle, (b) after 5 cycle, and (c) after 9 cycle.

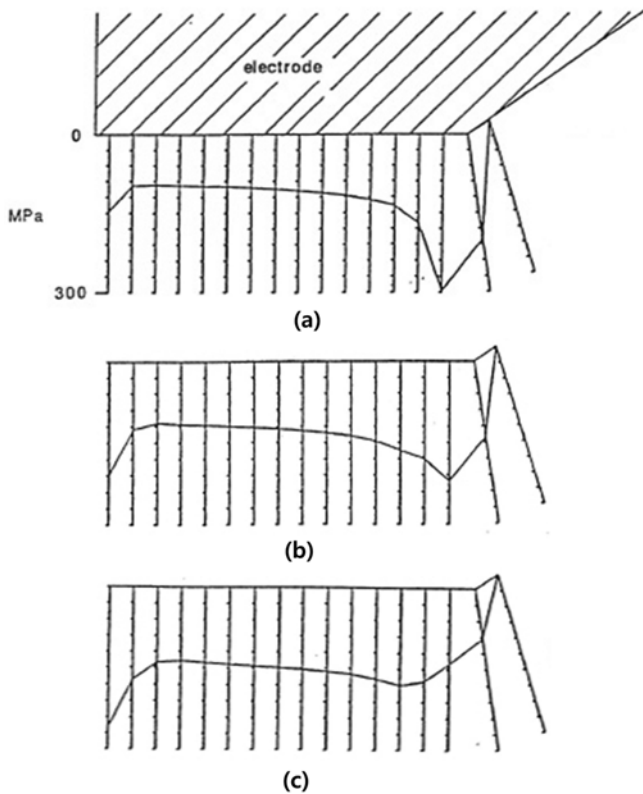


Fig. 6. Change of contact pressure at the electrode interface during welding. (a) after 1 cycle, (b) after 5 cycle, and (c) after 9 cycle.

to the electrode (within 0.15 second for this simulation case). After this time the contact size increases due to large deformations in the work piece. Severe indentation begins at this stage of welding.

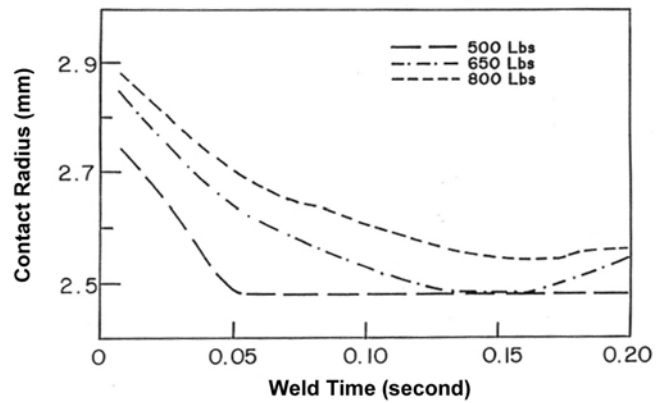


Fig. 7. Change of contact size at the faying interface during welding.

From this simulation it is seen that the current density at the faying interface changes significantly during the course of welding. The initially large contact area decreases as weld progresses due to thermal expansion and then increases again as mechanical collapse begins in the work piece due to the presence of molten metal. This can be related to the tailing of the lobe curve in the high current short weld time region. It was seen in reference 19 that welding with high current generally shows severe localization in the heat generation pattern [19]. This localized heating is combined with a very rapid expansion. In this case, the dissipation of heat from the localized hot spot is small due to the very short weld time. The localized thermal expansion may also cause loss of mechanical constraint of the nugget envelope due to the asymmetry of the process. Thus expulsion can occur before the formation of a proper nugget resulting in a small or negligible current range.

The zinc coated material will behave in a different way. The current conducting area is determined by the behavior of the zinc at the faying interface. Figure 8 shows the experimentally measured growth of nugget size and zinc halo during welding. The effect of increased current conducting

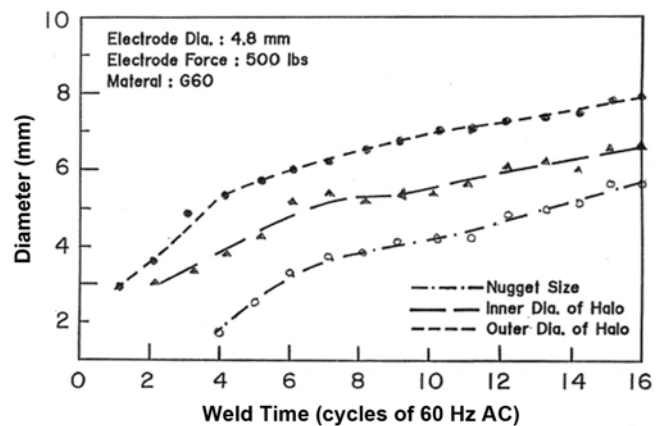


Fig. 8. Evolution of halo size and nugget size.

area in a zinc coated steel is very important on the nugget growth mechanism. As the current flow area increases at the faying interface, the heat generation rate decreases in a quadratic manner compared to the heat generation rate at the electrode interface. This implies that the temperature rise at the electrode interface is much more rapid than at the faying interface for coated steel. If the effect of current oscillation in AC welding is also considered, the amplitude of temperature fluctuation at the electrode interface can be even greater. This phenomenon will hinder the gradual formation of a nugget and will also make surface expulsion from the electrode interface easier.

### 3.2. Effect of changes in basic variables on nugget growth

The effect of variability in each parameter derived from Table 1 was numerically simulated to see the effect on the nugget growth behavior and thus to be used in determining the most important parameters in controlling nugget growth. The simulated material was an electrogalvanized low carbon steel AM68.

For a given variability in each parameter, the differences in weld time required for a nominal nugget size of 2.0 mm radius was estimated. The total range of variations in each parameter is double the variation of 5% in one direction. The difference between the upper and lower times to nugget formation was taken as a measure of change in nugget growth behavior. An increase in nugget development time results in a larger energy input requirement. This is equivalent to the requirement of higher weld current level. This difference is also representative of the lobe width. A large difference in weld time is equivalent to the larger lobe width on the current axis.

Figure 9, as an example, illustrates the simulation results of nugget growth behavior for the case of variations in electrode diameter. In this Fig. 9, 10% variation in electrode diameter resulted in 4.5 cycles of weld time change. As another example, Fig. 10 illustrate the effect of changes in the contact diameter at the faying interface. In this case 10% variation resulted in 2.5 cycle changes in weld time. In the same man-

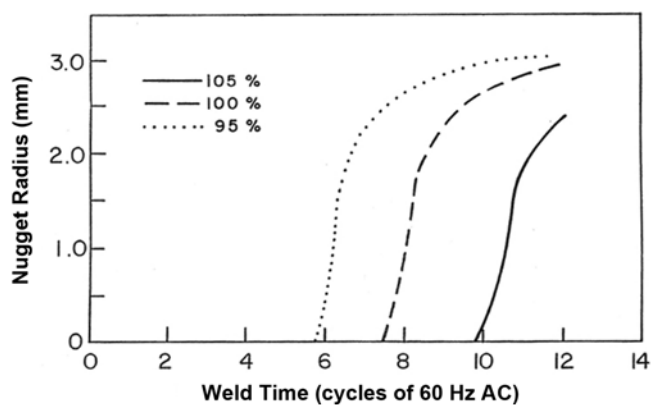


Fig. 9. Effect of changes in the electrode diameter.

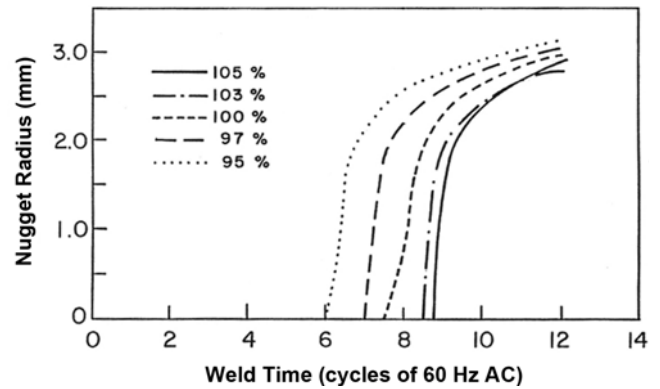


Fig. 10. Effect of changes in the contact diameter at the faying interface.

Table 5. Effect of changes in basic variables on nugget growth time

Increase in (by 10%)	Increase in nugget growth time (cycle)
Thermal conductivity, $k_b$	0.50
Specific heat, $\rho C_p$	0.75
Electrical resistivity, $\sigma_b$	-1.0
Specimen thickness, $L$	-0.25
Electrode radius, $b$	4.5
Contact radius, $D$	2.5
Contact resistance at faying interface, $R_c^f$	-0.001
Contact resistance, $R_c$	-0.126
Contact resistance at electrode interface, $R_c^e$	-0.125
Contact heat transfer coefficient, $h_c$	0.125

ner the effect of changes in each basic variables on the weld time were simulated. The results are summarized in Table 5. The discussion of the effect of changes in basic variables are discussed below.

#### 3.2.1. Effect of Material Related Variables

The thermal conductivity,  $k_b$ , electrical resistivity,  $\sigma_b$ , and heat capacity,  $\rho C_p$ , were varied in the model. The nugget formation starts later as thermal conductivity increases. The reason can be ascribed to a lower heat loss to the electrode and surrounding material. If heat conduction to the electrode is dominated by interface control, one cannot expect a strong effect of the thermal conductivity on nugget growth, particularly when the specimen is thin.

The materials with high electrical resistivity experience a faster heat build up in the nugget and complete nugget formation in less time. The reason of this increased sensitivity comes from the cumulative effect of electrical resistivity. As the electrical resistivity increases with temperature, for a material with higher initial electrical resistivity, the faster initial rise of temperature raises the resistance more rapidly and generates more heat. Thus the nugget growth curve will become steeper and produce shorter nugget development time. This phenomenon may not be beneficial in terms of stable nugget

growth. The slope of  $ds_b/dt$  has another very important effect in its contribution to the redistribution of the current. Due to the geometry of the welding system, the center part of the nugget is usually the highest temperature region. Thus the center part will have the highest electrical resistivity. The higher resistance at the center part will push the current to the periphery of the nugget, increasing the temperature in this peripheral region. Thus it is not clear whether the greater slope in temperature dependence of electrical resistivity is beneficial or not.

The effect of heat capacity is reversed, compared to the effect of resistivity. For an increase in specific heat, the time required to raise the work piece temperature to the melting temperature is longer. Since the temperature rise time is longer, the temperature field in the work piece has more chance to even out the temperature profile in the radial direction. Thus, once the nugget starts to form, the nugget can grow faster.

### 3.2.2. Effect of geometrically related variables

The nugget growth time was estimated for various size of electrode face radius,  $b$ , contact radius at the faying interface,  $D$ , and specimen thickness,  $L$ . The effect of electrode size is very strong, producing changes in nugget growth time of 4.5 cycles. This change may be great enough to make nugget formation impossible. However, the effect of variation in the work piece thickness is very small. As the thickness increases, the nugget forms earlier. Since the thicker material loses less heat to the electrode, more heat is available for nugget formation. This can be explained by the higher electrode temperature as measured in reference 17.

The contact size,  $D$ , includes the total area of the current path. It was seen in Figs. 7 and 8 that electrode force and zinc halo formation are the primary sources of changes in contact area at the faying interface. One interesting observation in these nugget growth curves is the varying effect of contact size. Decreasing contact size shows more significant changes in nugget development time than increasing contact size. Two reasons can be postulated. The first is the stronger effect of current redistribution when welding a material with small contact area. This was related to the temperature dependence of the electrical resistivity of the work piece. The other is the quadratic effect of the current density on the heat generation rate at the faying interface. This phenomenon makes the effect of contact area very significant in the nugget development mechanism.

If the contact size or the electrode size increases, the total resistance in the system will decrease due to increases in the current conducting area. This will reduce the welding current and the power absorbed by the work piece. Thus the increasing electrode size or the contact size will shift the nugget formation time a greater extent at longer weld times.

For a given material, the value for  $D/b$  is determined by the loading condition and the presence of a coating. As a general rule, a larger value of  $D/b$  will localize the heating of mate-

rial at the electrode interface and will make welding difficult. This is particularly true for welding of thin material. As the displacement induced by thermal expansion is cumulative in nature, the total thermal displacement of thin material at the center line is smaller than that of a thick material by roughly the ratio of specimen thickness. The smaller thermal displacement at the center of contact will make contact at the periphery easier. This results in a larger  $D/b$  value for thin materials. A larger value of  $D/b$  means that a greater percentage of the heat is generated at the electrode interface as opposed to the faying interface.

### 3.2.3. Effect of interface related variables

In Table 1, two parameter groups are listed as the electrical parameter and the thermal parameter. These basic parameters in each group are interface related parameters, i.e. electrical contact resistance at the faying interface,  $R_c^f$ , and at the electrode interface,  $R_c^e$ , contact heat transfer coefficient,  $h_c$ , at the electrode interface and the convective heat transfer coefficient at the coolant interface,  $h_w$ .

It was seen in reference 19 that the effect of coolant flow rate is small compared to the effect of electrode face thickness. The effect of flow rate becomes more important as the electrode thickness decreases. However, as the heat transfer at the coolant interface is another complicated boundary heat transfer problem, it was not included in this variability analysis [20].

One important aspect to be noted here is that the contact heat transfer coefficient at the electrode interface is coupled to the electrical contact resistance. This means that one cannot change the electrical contact resistance without affecting the thermal contact heat transfer coefficient. In this simulation, when the contact resistance at the electrode interface was increased, the contact heat transfer coefficient was decreased by the same percentage used for the change of resistance. Thus the effect of changes in contact resistance and contact heat transfer coefficient were considered to be the same but in opposite directions.

The simulation results showed that the change in the contact resistivity at the faying interface does not produce any significant change in nugget growth time. An effect can only be seen in the early stages of nugget growth. This can be ascribed to the rapidly decaying characteristics of contact resistance at the faying interface. This needs to be distinguished from the ease of welding of materials with high interface contact resistance at the faying interface. The effect of contact resistance changes at the electrode interface was more pronounced than the effect of changes at the faying interface, even though it is very small.

The effect of simultaneous changes both at the faying interface and at the electrode interface was also simulated to see the effect of changes in contact resistance,  $R_c$ , as a sum of contact resistances at the faying interface and at the elec-

trode interface. The results matched well with the combination of simulation results for faying interface change and those for electrode interface change. Thus far it is seen that a variation in the electrical contact resistances either at the faying interface or at the electrode interface has a small effect on the nugget growth curve.

### 3.3. Sensitivity of nugget growth curve to characteristic parameters

The data listed in Table 5 contain information about the sensitivity of nugget growth to variations in basic parameters. From this information Table 6 was constructed to see the effect of characteristic parameters on nugget growth time. Table 6 can be used as an index to ascertain the relative importance of these characteristic parameters and the effect of variations on weld time. In constructing this table it was assumed that the variation in the component is less than 10%, which was the range used in the simulation. Thus the results are only applicable to the particular case considered in this work.

For example, the effect of  $k_b/\sigma_b$  and  $\rho C_p/\sigma_b$  were calculated by considering the maximum possible range. If a 10% increase in  $k_b/s_b$  results from an increase in  $k_b$ , the increase in weld time will be 0.5. However if the 10% increase results from a 10% decrease of  $\sigma_b$ , the increase in nugget growth time becomes 1.0. Combining the effects of each variable in this manner, one can estimate a parameter index. This index can be used as a measure of the sensitivity of nugget growth to changes in the characteristic parameters.

Among all these characteristic parameters, the geometrical parameters show the strongest effects. Table 6 shows that the most important parameter is the ratio of contact size to the electrode size. The next is the ratio of electrode radius to the square of work piece thickness. The material parameters have intermediate importance. The electrical parameters and the thermal parameters show the least importance in this classification. This is true for the case of low carbon steel. However, if a larger variability of the electrical parameters and the thermal parameters is considered, these parameters can be more important than the other parameters. As an example, even though the effect of the geometrical parameter is the strongest, if the variability of this parameter is very small, the

effect of other parameters may become important.

### 3.4. Application example of sensitivity index

Welding of very thin zinc coated steel is known to be very difficult. This is believed to be due to the large  $b/L^2$  and  $D/b$  value. The lower value of  $R_c/R_b$  is another less important reason. As the thickness becomes less, more heat flows to the electrode. For ideal contact conditions this may help produce a sound nugget. In an ideal case, greater heat transfer to the electrodes will lower the work piece temperature at the electrode interface, making the temperature gradient in the axial direction steeper. This will help increase the temperature difference between the faying interface and the electrode interface. However as  $b/L^2$  becomes large, the temperature difference between the faying interface and the electrode interface becomes very small due to a smaller aspect ratio of the thickness to the contact radius. In addition, mismatched or tilted electrodes will localize the welding current distribution, resulting in a severely localized temperature. In the welding of thick material, this localization is believed to be dissipated very quickly due to the larger heat conduction path. For thin material, the conduction path is limited to two dimensions and rapid heat conduction from the hot spot is not possible. One good way to help reduce this problem is to increase the heat transfer coefficient at the electrode interface while increasing the electrical contact resistance at the faying interface.

In this respect, the ratio of contact resistance at the faying interface to the contact resistance at the electrode interface is a very important parameter in the welding of thin materials. The desirable heat distribution pattern is the one which has the highest temperature at the faying interface, particularly at the nugget center. It was also shown in the previous section that the effect of contact size at the faying interface is the major factor in determining the nugget growth characteristics. The larger contact area will reduce the current density at the faying interface and will prevent the nugget from growing in a gradual way. More heat will be generated at the electrode interface. Slower heating with a larger faying interfacial area decreases the temperature gradient in the radial direction and will make the nugget growth very abrupt.

To verify this concept an experimental lobe for 0.6 mm thick G40 material was produced. Figure 11 shows the lobe curve of the original material containing zinc on both surfaces. This lobe curve has only a 0.5 kA lobe width when welded with 8 cycles. Figure 12 shows the lobe of the modified material. The zinc coating at the faying interface was etched away leaving a bare steel surface, but the zinc at the electrode interface remained. The purpose was primarily to decrease the contact size at the faying interface rather than to increase the contact resistance. One has seen that the effect of the contact resistance is much less than that of the contact size. The result shows that the lobe width increases by more than 250%.

For better weldability of a thin material, it is necessary to

**Table 6.** Sensitivity index for the characteristic parameters

Increase in (by 10%)	Possible range of change in nugget growth time (cycle)
$k_b/\sigma_b$	0.5 ~ 1.0
$\rho C_p/\sigma_b$	0.75 ~ 1.0
$b/L^2$	0.125 ~ 4.0
$D/b$	-4.5 ~ 2.5
$R_c/R_b$	-0.126 ~ 1.0
$R_c^f/R_c^e$	-0.001 ~ 0.125
$h_c/R$	-0.125 ~ 1.126
$h_c/k_b$	-0.5 ~ 0.125

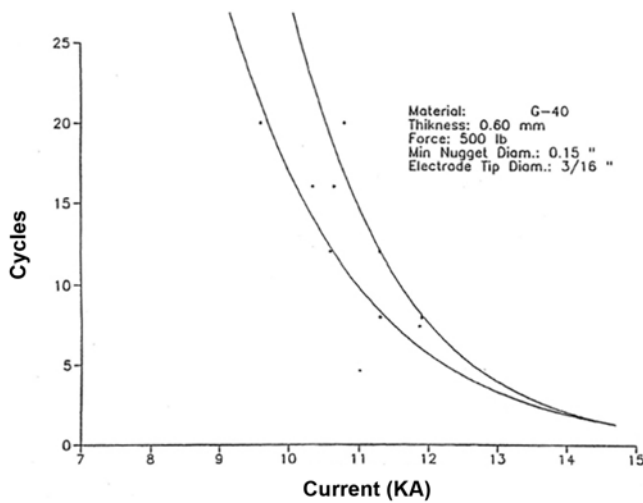


Fig. 11. Lobe curve of 0.6 mm thick G40 hot dip galvanized steel.

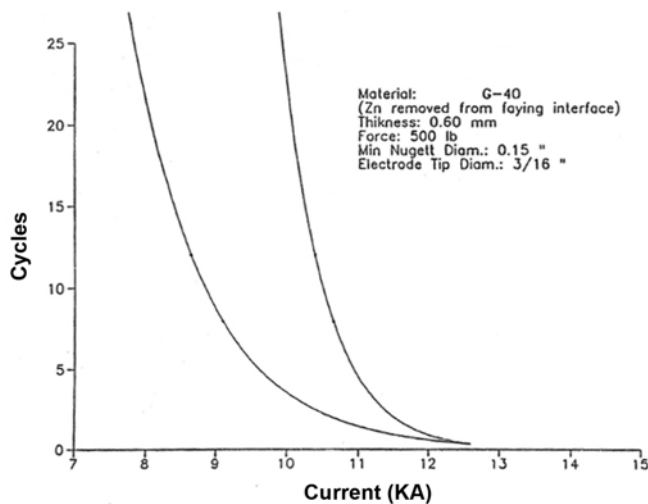


Fig. 12. Lobe curve of modified 0.6 mm thick G40 hot dip galvanized steel (coating only on the electrode side).

modify the axial temperature profile to produce a high temperature gradient. Two different methods can be contemplated in this respect: the first is modification of the faying interface. A reduction in contact area or an increase in the ratio of electrical contact resistance at the faying interface to the electrical contact resistance at the electrode interface is beneficial. The second is tailoring of the axial temperature profile by modifying the current wave form. In this case, heat is generated for a certain time and then the current is halted or reduced. The electrode interface cools down more quickly due to the heat sink of the electrodes and the faying interface maintains its heat and hence a higher electrical resistance. Then reheating follows with successive cooling. This cycle is repeated till formation of a nugget starts. This scheme should be coupled with a method which enhances the heat flow at the electrode interface. An electrogalvanized surface with a thick coating is a good candidate for this purpose. This

type of zinc coating has a smaller electrical contact resistivity. A reduction of contact size can be made as was done by using a bare steel surface at the faying interface. However this is not practical in terms of corrosion protection. Another possibility of decreasing the contact size is to use a galvanized surface at the faying interface. The contact heat transfer coefficient of galvanized steel has similar thermal contact characteristics as bare steel. For this reason the welding of galvanized steel is generally reported to have the welding characteristics of bare steel. Thus a material with an electrogalvanized surface at the electrode interface and a galvanized surface at the faying interface would be beneficial in improving the welding current range. In practice, this is not a very practical solution to improved weldability.

Changes in electrode size were the most influential among all the basic variables. An increase of 10% in the electrode radius, which is generally smaller than that commonly observed in actual welding, delayed the nugget formation by 4 cycles. This is large enough to make the nugget formation impossible under practical conditions.

#### 4. CONCLUSION

Understanding the fundamental phenomena of the resistance spot welding process is crucial to improve the process application. As a first step a lumped parametric model was developed to derive the characteristic controlling parameters. In this research, in order to quantify the sensitivity of nugget growth to changes in these parameters, a numerical model which incorporates the electrical, mechanical and thermal contact was developed. A sensitivity index table was constructed and analyzed to ascertain the relative importance of these characteristic parameters.

It was found that the most important factor in determining the variability of nugget growth behavior is the ratio of contact radius to electrode radius and the ratio of electrode radius to the square of specimen thickness. In general for a variation of 10%, the geometrical parameters are most important, followed by the material parameters. The electrical parameters and the thermal parameters are the least important.

It was also found that the ratio of contact radius at the faying interface to the electrode radius is about 1.2 at the start of welding and there is a pressure concentration at the periphery of the contact at the faying interface and at the edge of the electrode. However, the pressure concentration decreases as welding progresses, the contact size at the faying interface decreases resulting in very easy expulsion. The importance of contact at the faying interface is greater for the contact area than for the contact resistance. The contact area at the faying interface determines the current level and the ease of welding. The ease of spot welding of bare steel is due to the small contact size, not to the high contact resistance. A 0.6 mm thick galvanized sheet steel can be made more weldable through

making faying interface modification to have smaller contact size induced by a harder surface.

## REFERENCES

1. E. Kim, Sc.D., *Analysis of Resistance Spot Welding Lobe Curve*, pp.209-287, Massachusetts Institute of Technology, Cambridge, U.S.A. (1989).
2. E. W. Kim and T. W. Eagar, *SAE Transactions*, **No. 880278** (1988).
3. T. Horita, M. Oka, T. Kanamura, K. Yamazaki, and T. Fujiwara, *Welding International* **10**, 937 (1996).
4. A. Aravinthan and C. Nachimani, *Welding Journal* **90**, 143s (2011).
5. W. L. Chuko and J. E. Gould, *Welding Journal* **81**, 1s (2002).
6. X. Sun, E. V. Stephens, M. A. Khaleel, H. Shao, and M. Kimchi, *Welding Journal* **83**, 188s (2004).
7. S. Boron, *Welding International* **12**, 932 (1998).
8. C.-W. Ji, I. Choi, Y. D. Kim, and Y.-D. Park, *Korean J. Met. Mater.* **52**, 931 (2014).
9. Md. A. M. Hossain, Md. T. Hasan, S.-T. Hong, M. Miles, H.-H. Cho, and H. N. Han, *Met. Mater. Int.* **19**, 1243 (2013).
10. S. J. Na and S. W. Park, *Welding Journal* **75**, 233s (1996).
11. X. Sun, *Welding Journal* **79**, 244s (2000).
12. X. Sun and M. A. Khaleel, *Welding Journal* **83**, 197s (2004).
13. D. J. Browne, H. W. Chandler, J. T. Evans, P. S. James, J. Wen, and J. Newton, *Welding Journal* **74**, 417s (1995).
14. H. A. Nied, *Welding Journal* **63**, 123s (1984).
15. W. Zhang, *Welding in the World* **50**, 29 (2006).
16. Y. S. Zhang, J. Xu. M. Lai, and G. L. Chen, *Science and Technology of Welding and Joining* **13**, 192 (2008).
17. K. S. Yeung and P. H. Thornton, *Welding Journal* **78**, 1s (1999).
18. E. Kim, *International Journal of Korean Welding Society* **2**, 1 (2002).
19. E. W. Kim and T. W. Eagar, *Welding Journal* **68**, 303s (1989).
20. Z. H. Rao, S. M. Liao. H. L. Tsai, P. C. Wang, and R. Stevenson, *Welding Journal* **88**, 111s (2009).